Ecological Modelling 476 (2023) 110226

Contents lists available at ScienceDirect

Ecological Modelling

journal homepage: www.elsevier.com/locate/ecolmodel

An eco-epidemiological model supporting rational disease management of *Xylella fastidiosa*. An application to the outbreak in Apulia (Italy)

Gianni Gilioli [a], Anna Simonetto [a,*], Michele Colturato [a], Noelia Bazarra [b], José R. Fernández [b], Maria Grazia Naso [a], Boscia Donato [c], Domenico Bosco [d], Crescenza Dongiovanni [e], Andrea Maiorano [f], Olaf Mosbach-Schulz [f], Juan A. Navas Cortés [g], Maria Saponari [c]

[a] *Dipartimento di Ingegneria Civile, Architettura, Territorio e Ambiente e di Matematica, Università di Brescia, Italy*
[b] *Departamento de Matemática Aplicada I, Universidade de Vigo, ETSI Telecomunicación, Campus As Lagoas Marcosende s/n, Vigo, 36310, Spain*
[c] *Consiglio Nazionale delle Ricerche, Istituto per la Protezione Sostenibile delle Piante, Sede Secondaria di Bari, Italy*
[d] *Dipartimento di Scienze Agrarie, Forestali e Alimentari, Università degli Studi di Torino, Largo Paolo Braccini, 2, Grugliasco, 10095, Italy*
[e] *Centro di Ricerca, Sperimentazione e Formazione in Agricoltura Basile Caramia, Locorotondo, Italy*
[f] *European Food Safety Authority, Parma, Italy*
[g] *Instituto de Agricultura Sostenible (IAS), Consejo Superior de Investigaciones Científicas (CSIC), Avda. Menéndez Pidal s/n, Córdoba, 14004, Spain*

ARTICLE INFO

Keywords:
Mechanistic model
Short-range spread
Olive trees
Bacterium
Pathosystems
Eradication strategies

ABSTRACT

Knowledge on the dynamics of *Xylella fastidiosa* infection is an essential element for the effective management of new foci. In this study, we propose an Eco-epidemiological Model (XEM) describing the infection dynamics of *X. fastidiosa* outbreaks. XEM can be applied to design disease management strategies and compare their level of efficacy. XEM is a spatial explicit mechanistic model for short-range spread of *X. fastidiosa* considering: i) the growth of the bacterium in the host plant, ii) the acquisition of the pathogen by the vector and its transmission to host plants, iii) the vector population dynamics, iv) the dispersal of the vector. The model is parametrized based on data acquired on the spread of *X. fastidiosa* subsp. *pauca* in olive groves in the Apulia region. Four epidemiological scenarios were considered combining host susceptibility and vector abundance. Eight management strategies were compared testing several levels of vector control efficacy, plant cutting radius, time to detection and intervention. Simulation results showed that the abundance of the vector is the key factor determining the spread rate of the pathogen. Vector control efficacy and time to detection and intervention emerged as the key factors for an effective eradication strategy. XEM proved to be a suitable tool to support decision making for the drafting and management of emergency plans related to new outbreaks.

1. Introduction

Xylella fastidiosa (*Xf*) is a xylem-limited gram-negative bacterium originating from the Americas, identified in Europe during the last decade when the Italian authorities reported the first outbreak of *Xf* subsp. *pauca* in the south of the Apulia region in 2013. Afterward, the bacterium has also been detected in France (first outbreak in Corse, 2015), Switzerland (detected in 2015, now eradicated), Spain (first outbreak in Balearic islands, 2012), Germany (an isolated infection in 2016 now eradicated), and Portugal (first outbreak in Porto, 2019) (EFSA PLH Panel, 2019; EPPO Reporting Service, 2018; EPPO Reporting Service, 2019).

In Europe, the bacterium represents a significant risk for several crops and therefore a serious threat to food security (EFSA PLH Panel, 2020; Schneider et al., 2020). Host plants, susceptibility and symptoms vary according to the *Xf* subsp./strains (Nunney et al., 2013; Sanderlin, 2017).

Several important crop diseases can be associated with *Xf*, such as the Pierce's disease of grapevine, the plum leaf scald, the Citrus variegated chlorosis, the phony peach disease, and as confirmed in Italy, *Xf* is the cause of olive quick decline syndrome, which dramatically brought the Apulia olive growing sector to its knees (Hopkins and Purcell, 2002; Saponari et al., 2017).

The bacterium is transmitted by xylem-sap feeding insects (Almeida et al., 2005; Perring et al., 2001; Purcell et al., 1999; Redak et al., 2004). Host species and bacterium strains highly influence vector competence

* Corresponding author.
E-mail address: anna.simonetto@unibs.it (A. Simonetto).

https://doi.org/10.1016/j.ecolmodel.2022.110226
Received 27 March 2022; Received in revised form 3 November 2022; Accepted 15 November 2022
Available online 28 November 2022

(Cavalieri and Porcelli, 2017; Lopes et al., 2009). In Europe, *Xf* is mainly transmitted by the indigenous vector *Philaenus spumarius* (Cornara et al., 2018; Cruaud et al., 2018; Moralejo et al., 2019). More recently, two other spittlebug species, *Philaenus italosignus* and *Neophilaenus campestris,* have also been identified as competent vectors (Cavalieri et al., 2019).

The *Xf* epidemiological system is characterized by high variability and heterogeneity according to prevalence and spread of the infection (Sicard et al., 2018; EFSA PLH Panel 2019). The spatial and temporal patterns of disease dynamics strictly depend on the interactions among bacteria, vectors, and host plants in the pathosystem. These interactions are mediated by complex physiological and pathological processes and strongly influenced by environmental variables (e.g., temperature, water stress) (Almeida et al., 2005; Cornara et al., 2017; Jeger and Bragard 2019).

Several models have been proposed to investigate the key factors determining the *Xf* dynamics and how to manipulate them to support disease management (Parnell et al., 2017). Focusing on process-based models, a wide variety of approaches can be found in the literature: reaction-diffusion models (Chapman et al., 2015), susceptible-exposed-infectious-removed (SEIR) models (Jeger and Bragard, 2019; White et al., 2020), lattice susceptible, infected, removed (SIR) models (Fierro et al., 2019), spatially-explicit simulation models, short-distance deterministic and long-distance stochastic kernels (White et al., 2017), discrete-time versions of standard differential equations used in epidemiological compartmental models (White et al., 2019), and ordinary differential equation systems (Brunetti et al., 2020). Despite the variety of models proposed, there is still the need to further explore the epidemiology of *Xf* by integrating biological elements influencing the *Xf* disease spread and growth mechanisms and patterns.

To contribute to the effort of developing integrated modeling approaches, in view also of the need of supporting rational disease management, we propose a *Xf* Eco-epidemiological Model (XEM) describing the continuous spread of *Xf* in an area. XEM is a spatially explicit mechanistic model considering the following biological processes: i) the growth of the bacterium into the xylem of the host plant, ii) the acquisition of the pathogen by the vector from an infected plant, and its transmission to healthy plants, iii) the basic elements of the vector population dynamics, iv) the dispersal of the vector. The environmental drivers affecting *Xf* epidemic dynamics are considered in the model in terms of the impact on both the vector population dynamics and the development of the bacterial population in the host plant. XEM describes the spatio-temporal dynamics of the disease and the vector in a continuous or patchy landscape, with any composition of the plant community.

Through the description of the landscape structure and the accurate calibration of the functions' parameters, XEM can easily be adapted to describe any specific context and management strategies. XEM is a suitable tool to evaluate the effectiveness of different risk reducing options and practices aimed to the management of the disease pressure and spread, as well as to compare the efficacy of strategies aimed at the eradication of new outbreaks.

In Section 2.1 we describe the mathematical formulation and the biological assumptions of XEM. In Section 2.2 we apply the model to the Apulia outbreak of *Xf*, therefore the model components and the parameterization for the case study are presented. The management strategies and scenario analysis approach are explained in Section 2.3. The results of the scenario analysis on infection spread and management strategies are reported in Section 3. Discussion and conclusion are presented in Section 4.

2. Materials & methods

2.1. Mathematical formulation

XEM describes the spread dynamics of *Xf* in a spatial domain (Ω) during the time interval $[0, T]$. XEM is based on the following biological assumptions:

- The univoltine biological cycle of the vector *P. spumarius* is here simplified considering two phenological stages: the pre-imaginal stage and the adult stage. The two stages do not overlap. In XEM, an adult vector can become infected solely by feeding on an infected plant. Once infected, the vector can transmit the bacterium feeding on other plants, infecting and/or re-infecting (i.e., increasing the bacteria load) them. The pre-imaginal stage is not able to acquire neither to transmit the bacterium.
- Vector population dynamics are represented in a simplified way, the phenological processes and events are described as occurring at predefined times in the year, depending on the site under consideration. Change in population abundance is described only for the adult stage by means of a site-specific natural mortality function. The initial conditions for the adult stage are set equal to a site-specific maximum abundance interpreted as the local population carrying capacity. If no external mortality factor is applied (e.g., per-imaginal or adult control), each year adult population dynamics has the same initial conditions, this assumption corresponds to the case in which adult fecundity exactly compensates pre-imaginal mortality.
- Vectors move in the spatial domain. Only individuals in the adult stage can disperse and the dispersal behavior is modelled by means of a random walk motion. Vector long-distance dispersal due to both human-assisted or natural movement is disregarded.
- The health status of a plant is described by the bacterial load titre in the xylem. In an infected plant, the bacterial load titre grows due to the multiplication of the bacterial population within the plant. A plant can receive multiple successful inoculums of the disease pathogen due to the feeding of the infected vectors. These multiple inoculums also contribute to bacterial population growth. We disregard plant mortality depending on bacterial load, therefore for a high level of bacterial load titre the plant remains a source of bacteria for adult vectors. This simplified assumption can be acceptable for a relatively short time period relevant for management consideration, as considered in this paper.
- Successful transmission of the pathogen to the host plant is described by a transmission function that considers: (i) the vector feeding behavior (also including the vector preference for the target host), (ii) the capacity of the vector to transmit the pathogen, (iii) the susceptibility (s) of a specific host plant (species or cv) to the pathogen. The possibility that vectors take and spread the disease is influenced by the bacterial titre in the host plant.
- XEM considers only the short-range spread of the disease. We assume the disease to propagate solely by the natural local dispersal and the feeding activities of the vectors. Long jumps of the disease, due to natural or human-assisted dispersal of infected vectors, or to the trade of infected plant material are not included in the model.

The model state variables are

- The abundance of infected adult vectors in the spatial point x at time $(\gamma(x,t))$. The variable $\gamma(x,t)$ assumes values in the range $[0, A(x,t)]$, where $A(x,t)$ is the adult vector abundance. The abundance of uninfected adult vectors can be calculated as the difference between the vector population abundance and the abundance of infected vectors $(A(x,t) - \gamma(x,t))$. $\gamma(x,t)$ is equal to 0 during the pre-imaginal stage.
- The health status of a host plant in the spatial point x at time t $(\varphi(x,t))$. The health status of a host plant represents the level of bacteria load in that plant at time t, and it assumes values in the range $[0, 1]$ as it is normalized to a maximum level of bacteria load (see Table 3). In a non-infected plant, the bacterium is absent, therefore $\varphi(x,t) = 0$. In an infected plant, $\varphi(x,t)$ is greater than 0 and proportional to the bacteria load in the plant.

For the sake of clarity, hereinafter, $\varphi(x,t)$ and $\gamma(x,t)$ will be reported without their parameters.

The spread in space and time of the disease is described through a nonlinear system composed of a parabolic partial differential equation for γ and a first-order ordinary differential equation for φ:

$$\dot{\gamma}(x,t) = d\Delta\gamma(x,t) - M\gamma(x,t) + b(x,t)(A(x,t) - \gamma(x,t))\varphi(x,t) \quad (1)$$

$$\dot{\varphi}(x,t) = [s\ l(x,t)\ \gamma(x,t) + F(t)\varphi(x,t)](1 - \varphi(x,t)) \quad (2)$$

$$\partial_\nu \gamma(x,t) = \nabla\gamma(x,t)\cdot\upsilon(x) = 0$$

$$\varphi(x,0) = \varphi_0(x),\ \gamma(x,0) = \gamma_0(x)$$

where Δ is the Laplacian operator, ν is the normal versor on the boundary of Ω, ∂_ν stands for the outward normal derivative on the boundary of Ω, $\varphi_0(x)$ and $\gamma_0(x)$ are the initial conditions, i.e., the status of the system at $t = 0$. The parameters of the XEM are defined in Table 1. The biological meaning of the parameters and their estimation are reported in Section 2.2.

The spatial domain Ω is approximated with a grid (mesh), considering the discrete counterpart of Neumann homogeneous boundary conditions on the discrete scheme (Brezis, 1986). The structure of the mesh is defined according to the characteristics of the landscape considered. In a continuous and homogeneous landscape, the host plants are placed in the nodes of the mesh and arranged in a continuous space with regular or irregular space among plants. In a patchy landscape, the host plants are present in restricted areas surrounded by unsuitable habitats or plants for the bacterium. This patchy spatial configuration can support metapopulation analysis of disease dynamics. Vectors are present in the whole Ω and the vector stage varies in time according to vector phenological dynamics.

Mathematical and numerical analysis of the model is detailed in Bazarra et al. (2022). Since we assume that functions $b(x,t)$ and $l(x,t)$ are positive, globally bounded and Lipschitz-continuous, the same existence, uniqueness and regularity properties still hold for the solution of system proposed in Bazarra et al. (2022).

Table 1
Parameters of the XEM.

Parameter	Name	Units	Description
d	Spread parameter of the vector	Spatial unit^2 time^{-1}	Parameter of the Laplacian operator related to the dispersal capacity of the vector
M	Natural mortality of the infected vector	Time^{-1}	Mortality rate in the survival function of the infected vector population
b	Acquisition rate function of the vector	Time^{-1}	Acquisition rate of bacteria by the vectors feeding on infected plants
$A(x,t)$	Vector population abundance	Pure number	Population abundance of adult vectors (infected and non-infected) at time t in a spatial unit x
s	Plant susceptibility rate	Time^{-1}	Probability in the time unit that a not-infected susceptible plant becomes systematically infected after the inoculation of bacteria by an infected adult vector during a day
$l(x,t)$	Bacterium inoculum	γ^{-1}	Bacteria load transmitted by a single vector in a successful feeding on a plant in a day
$F(t)$	Bacterial population growth function	Time^{-1}	Time-dependent bacterial population growth rate in infected plants

2.2. Model application

XEM is applied to the current epidemics of *Xf* subsp. *pauca* in olive groves in the Apulia Region (Southern Italy). In 2013, *Xf* was identified in the Salento peninsula, near Lecce in the southern part of the Apulia, where it infected millions of olive trees and caused the death of many of them. At the beginning of 2019, the *Xf*-infected area included approximately 718,000 ha in the Apulia Region (Saponari et al., 2019a; REGULATION, 2020b). The spread of *Xf* is still ongoing, seriously threatening the Apulian olive sector.

Results of scientific studies conducted in the context of the Apulian olive groves are used for estimating model functions and parameters related to the growth functions of the bacterium, the development of symptoms, the susceptibility of the different cultivars, and the phenology of the vectors. In the model application, the meadow spittlebug *P. spumarius* is considered the vector of *Xf*. To compensate for the lack of experimental data regarding the other functions and parameters of the model, we referred to data in the EFSA Update of the scientific opinion on the risks to plant health posed by *Xylella fastidiosa* in the EU territory (2019).

2.2.1. Landscape structure

Apulia is characterized by large olive groves with olive trees planted generally at large distances (e.g., 6- 10 m) (Strona et al., 2017). We represented this landscape by defining a homogenous mesh of 10 km x 10 km with equally spaced host plants. The nodes of the mesh are the spatial units and represent cells of 10 × 10 m. At the center of the node, there is a susceptible olive tree. We assumed the herbaceous cover between the hosts as not susceptible (Fig. 1) so only olive-to-olive transmission is considered.

In this work, we explored different disease dynamics scenarios by applying XEM with different plant physiological responses and vector population abundance (Di Serio et al., 2019). Since the situation in the Apulian infected area is characterized by homogeneous fields cultivated with a predominant olive cultivar, within a simulated scenario the host plants' susceptibility is set equal for all nodes. The typical agroecological conditions in the Apulian olive growing region are included in the model. The time step of the simulations is set to 1 day and the time horizon to 5 years.

2.2.2. Vector phenology and survival

The pre-imaginal stage occurs from the beginning of the year (t_i) up to the appearance of the adult stage (t_{V_i}) and after oviposition (t_{V_f}) until the end of the year (t_f) (Fig. 2). The adults emerge from pre-imaginal stage and occurs in the time interval $[t_{V_i}, t_{V_f}]$. In the this time interval, the adults population abundance varies according to the survival profile $A(x,t) = k_{max,y} * \sqrt{\frac{t_{V_f} - t}{t_{V_f} - t_{V_i}}}$, starting from the site-specific maximum carrying capacity $(k_{max,x})$ at t_{V_i}. In the time interval $[t_{V_i}, t_{V_f}]$, the abundance of infected adults is defined by $\gamma(x,t)$.

Based on the climatic conditions of Apulia and the data on adults emergence available in the literature (Bodino et al., 2020; Di Serio et al., 2019), we set $t_{V_i} = 130$ (May 10th) and the end of period of vector feeding activities at $t_{V_f} = 300$ (October 27th).

The natural mortality rate of the infected adults (the parameter M in Eq. (1)) has been estimated equal to 0.015 day^{-1}. This value describes a survival curve that well approximates available data on the duration of the adult stage and the population abundance of *P. spumarius* (Bodino et al., 2019; Bodino et al., 2021; Di Serio et al., 2019).

2.2.3. Vector dispersal

Only vectors in the adult stage can disperse. Their dispersal behavior is modelled by means of a random walk motion through the Laplace operator Δ and its diffusive coefficient d in Eq. (1). For the vector dispersal capacity, we referred to the median dispersal distance of

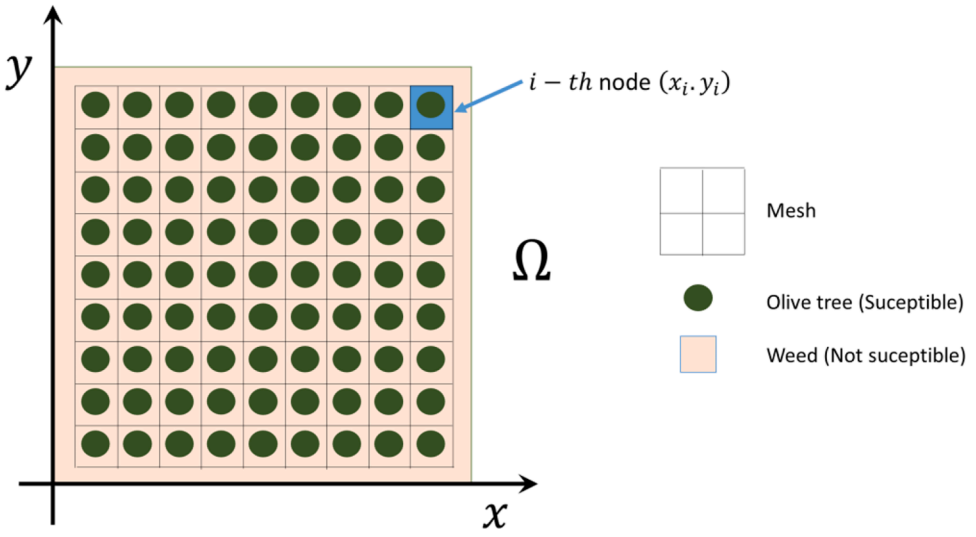

Fig. 1. Structure of the generic homogeneous landscape Ω configured to simulate the disease dynamics in the conditions of Apulian large olive groves. Host plants (green circle) are equally spaced defining a regular grid (black matrix). A non-susceptible weed covers the space between hosts.

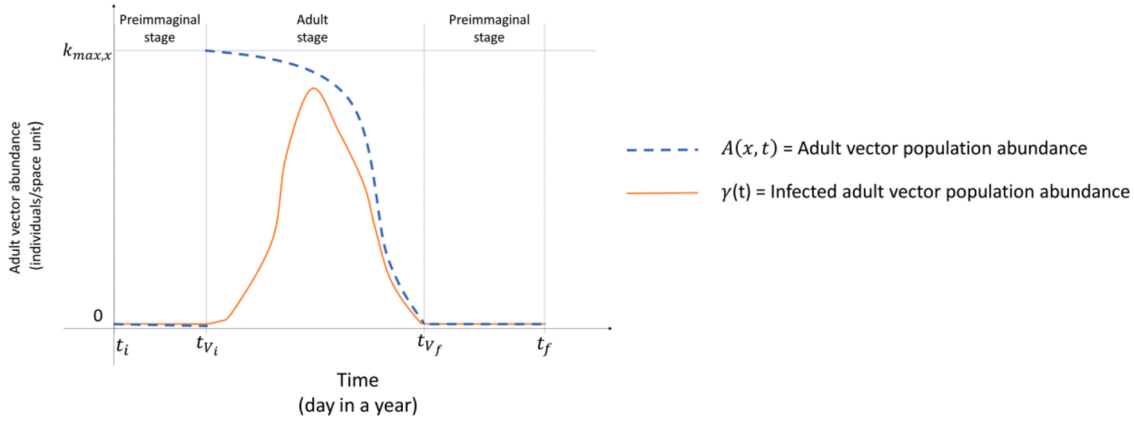

Fig. 2. Exemplification of the dynamics of infected vector abundance in 1 year of simulation where $t_i = 1$ is the first day of the year, t_{V_i} is the day of adult emergence, t_{V_f} is the day when the last adult disappears, and $t_f = 365$ is the last day of the year.

P. spumarius, estimated by EFSA equal to 800 m/year (EFSA PLH Panel, 2019). The value of the diffusive coefficient d is derived using a simulation procedure. An initial population of 1000 adult vectors is released in the center of the landscape at time t_{V_i}. We selected the value of d such that at t_{V_f} half of the vector population is in a circular area of 800 m of radius from the point of release. The estimated value of the parameter is $d = 1500\text{m}^2\text{day}^{-1}$.

2.2.4. Bacteria acquisition rate

To estimate the vector bacteria acquisition rate $b(x,t)$ (Eq. (1)) we referred to the median value (12.08%) of the elicited distribution of acquisition rates of the vector reported in the EFSA Opinion (EFSA PLH Panel, 2019), representing the daily probability of acquisition of the bacteria in optimal conditions (e.g., the vector feeds on highly infected plants only). In XEM, the acquisition rate of the vector in the EFSA Opinion is used to estimate the maximum value for $b(x,t)$ (b_{max}), achievable when $\varphi = 1$. To estimate b_{max}, a population of 1000 non-infected vectors feeding on highly infected host plants is simulated. After one day of feeding activity, we obtained 12.08% of the vectors infected with $b_{max} = 0.0995\ day^{-1}$.

In XEM, b_{max} is scaled according to the health status of the plant. We assumed that the probability of a successful daily feeding activity depends both on the bacterial titre in the plant and on the time spent in the feeding activity by the vector in a day. To represent this process, we used the Ivlev model (Ivlev, 1961), a non-linear functional response widely used to describe the predator's efficiency in searching and capturing the prey as a function of prey density: $p(x) = q * (1 - e^{-j\,p})$. In XEM, we set $= \varphi$, $q = b_{max}$, and $j = 50$. We select the value of j such that the bacteria acquisition rate is close to b_{max} when $\varphi(x,t) = 0.1$, corresponding to a symptom's severity in the host plant equal to three (see Table 3).

2.2.5. Bacterial population growth function

The bacterial population in an infected plant increases following the function $F(t)$ (Eq. (2)). Bacterial population growth varies according to the physiological state of the plant, the environmental conditions, and plant susceptibility.

Concerning plant physiology and environmental conditions, three periods in a year are identified: i), the physiological state of the host plant is not favourable to bacterial growth, so $F(t) = 0$, ii) the host is in a favourable physiological state for the bacteria, but the growth is sub-optimal due to not favourable environmental conditions (e.g., high temperature and low relative humidity), so the bacterial population grows at a low rate, $F(t) = r_L$, iii) both the host physiological state and the environmental conditions are favourable, the bacterial population grows at a high rate, $F(t) = r_H$. The bacterial population growth function is defined as follows:

$$F(t) = \begin{cases} 0 & t \in [1, t_{H_1}) \cup [t_{H_4}, 365] \\ r_H & t \in [t_{H_1}, t_{H_2}) \cup [t_{H_3}, t_{H_4}) \\ r_L & t \in [t_{H_2}, t_{H_3}) \end{cases} \quad \text{with } 1 < t_{H_1} < t_{H_2} < t_{H_3} < t_{H_4} < 365.$$

For the Apulian case, we set $t_{H_1} = 129$ (May 8th), $t_{H_2} = 212$ (July 29th), $t_{H_3} = 242$ (August 29th), $t_{H_4} = 287$ (October 12th). Growth rates depend also on the host plant susceptibility (Giampetruzzi et al., 2016; Saponari et al., 2019b). We used data from a field study on the dynamics of *Xf* spread and symptoms development, conducted in Apulia in 2016 and 2017 (Montes-Borrego et al., 2017), to derive the growth rates for different periods in the year and hosts susceptibility. We considered a susceptible olive tree cultivar (Ogliarola) and a tolerant cultivar (Leccino). The best estimates for the bacteria growth functions (Table 2) are obtained starting from an initial bacteria inoculum $\varphi_i = 0.0001$. In the Apulian datasets, a percentage of host-plants tolerant to infection (N_S) throughout all the observation period is reported. This cultivar-dependent percentage (Table 2) has been considered in the model.

2.2.6. Plant susceptibility

According to EFSA (2019), plant susceptibility is defined as the probability that a non-infected susceptible plant becomes systematically infected as a consequence of the feeding activity of an infected adult vector during a day. We set the plant susceptibility (s) for tolerant host plant equal to the first quartile of the distribution for susceptibility elicited by EFSA (2019) ($s = 0.09$), and to the median value of that distribution for susceptible host plants ($s = 0.14$).

2.2.7. Bacteria transmission to the plant

Infected vectors inoculate the bacteria into the host by feeding on the xylem-sap of the plant. In a plant not yet infected, bacteria inoculum triggers the process of plant infection. The bacteria inoculum per vector in a day is estimated equal to $l = 1 * 10^{-4}$, based on field studies on the dynamics of symptoms development *Xf* (Montes-Borrego et al., 2017).

In XEM, the transmission of the bacteria from the vector population to the host plant population takes into account a density-dependent reduction ($l(\cdot) = l * e^{-4\gamma}$) with the increase of vector population, estimated based on results obtained by Montes-Borrego et al. (2017). This is to account for both the increase of the probability of vector feeding in already infected leaves of the host plants and the effects of intra-species competition, leading to the selection of host plants other than olive trees.

2.2.8. Symptoms severity

We assume that during the asymptomatic period the plant is infected and infectious, but it does not manifest any visual symptoms. To correlate the level of infection of the plant $\varphi(t)$ with the severity of the symptoms, we referred to Saponari et al. (2019a) . These authors tested bacterial population load (C) for Ogliarola and Leccino cultivars and reported the estimation of symptoms severity, measured on a 6-points scale (0 - no symptoms; 5 -maximum level of symptoms, i.e., the plant is no longer productive). In Table 3, we report the thresholds of bacteria load and the corresponding values of plant health status for each class of symptoms severity.

Table 2
Estimates of the percentage of not susceptible plants, and of the high and the low bacterial population growth rates for the susceptible host plants (cv Ogliarola) and the tolerant host plants (cv Leccino).

	Percentage of not susceptible plants N_S	High growth rate r_H	Low growth rate r_L
Susceptible host plants (cv Ogliarola)	7%	0.020	0.010
Tolerant host plants (cv Leccino)	0.287	0.017	0.009

Table 3
Intervals of bacteria load (LogC) and plant health status ($\varphi(t)$) for the six symptoms severity classes.

Bacteria load *LogC*	Plant health status φ (t)	Plant symptoms severity
0	0	0
0 – | 5.06	0 – | 0.0115	1
5.06 – | 5.55	0.0115 – | 0.0352	2
5.55 – | 6.03	0.0352 – | 0.107	3
6.03 – | 6.52	0.107 – | 0.328	4
6.52 – | 7.00	0.328 – | 1	5

2.3. Simulation of epidemiological scenarios

The XEM, parameterized as in Section 2.2., is applied to explore the spatio-temporal dynamics of *Xf* considering two levels of vector abundance (high and low) and two levels of host plant susceptibility (high and low) (Table 4). Based on data published in Di Serio et al. (2019), we defined 20 adults per m^2 as the high level of vector population and 1 adult per m^2 as the low level of the vector population.

The onset of infection is simulated through the successful inoculation of nine susceptible plants in an area of 30 m radius in the center of a free area (inoculation point). Disease dynamics are analysed for 5 years, with a temporal resolution of 1 day.

The spatio-temporal dynamics of the disease in the four scenarios are assessed at the end of each simulation year according to the following output variables:

- Infected host plants: Number of infected host plants;
- Disease pressure: Mean value of health status of the host plants (φ). The mean is computed only on infected plants, i.e., $\varphi > 0$;
- Infected vector pressure: Mean annual density of the population abundance of infected vectors. The mean is calculated only during the period of adult presence;
- Disease spread: Maximum distance of the infected plants from the inoculation point.

The simulations were conducted in Matlab (version R2018b), applying the finite element approach to discretization (further details are reported in Bazarra et al., 2022).

2.4. Simulation of management scenarios

The definition of the management strategies to be tested is based on the European Legislation in force at the time the study was carried out (Council Directive 2000/29/EC, 2000; Decision (EU) 2015/789, 2015; Decision (EU) 2017/2352, 2017), focusing on eradication measures.

In our study, the management strategies are applied from the first detection of an infected plant in a free area (i.e., an area where infected

Table 4
Parameter used in the definition of the four simulation scenarios on epidemiological dynamics of *Xf* in Apulia olive groves.

Epidemiological Simulation Scenario (Epidem)		**Density of vector population** **High** (20 adults/m^2)	**Low** (1 adult/m^2)
Susceptibility of the host plant	**High** $s = 0.14, r_H = 0.02$; $r_L = 0.01$	Epidem-HH	Epidem-HL
	Low $s = 0.09, r_H = 0.017$, $r_L = 0.009$	Epidem-LH	Epidem-LL

plants are not reported) till the end of the simulation period. Following the detection of an infected plant, three areas are marked out around the detection point (area demarcation process). The first area, with a radius equal to the value of the cutting radius, is defined as the infected area. The second area is a circular crown with a minimum radius equal to the cutting radius and a major radius of 5000 m and is defined as the buffer zone. The infected area and the buffer zone constitute the demarcated area. Immediately after the detection, all potential *Xf* host plants are cut and one adult vector control treatment is performed in the infected area. In the years following the detection till the end of the simulation period, the management strategy applied in the demarcated area consists of one weed treatment, carried out in spring to control the nymph population, and two vector control treatments, carried out in late spring and in the summer. The vector control treatments have the aim of reducing both the adult vector population in the current year and the vector population in the next year, as a result of a reduction in the number of adults and then in the number of overwintering eggs that are laid. Therefore, the repetition of treatment over years leads to a significant reduction in the abundance of the vector. Fig. 3 graphically represents the management scheme applied in the scenario analysis. The sequence and type of control treatments to be performed are different in the first year of detection than in subsequent years because it is not possible to carry out weed treatment for nymphs control in the first year of detection. Management strategies are applied for 5 years.

Based on the overall structure of the management strategies described in Fig. 3, four factors relevant to eco-epidemiological dynamics and of interest to international policymakers are tested: efficacy of adult vector and weed control actions, the radius of the cutting area, time of the first detection, time to intervention. For each factor two levels are tested, defining a total of 16 management scenarios. Low efficacy of control treatments corresponds to 60% of nymph mortality following weeds treatments and 50% of adult mortality following chemical control of the adults, while high efficacy corresponds to 80% of nymph mortality following weeds treatments and 90% of adult mortality following chemical control of the adults. The large cutting radius corresponds to 100 m, the small cutting radius is set to 50 m. Two times for the first detection were considered: early and late detection occurs 3 and 4 years after inoculation, respectively. Finally, we tested the impact of two different implementation times of the control actions. Early and late intervention occur 30 and 60 days after the detection, respectively. The early intervention corresponds to the first period of adult flight (just after adults' emergence).

The efficacy of the management strategies scenarios was assessed by considering the characteristics of the worst-case scenario, i.e., the eco-epidemiological scenario where at the 5th year after infection the infected area was greater. The management strategies were applied for 5 years, including the years of the first detection. At the end of the simulation, the *Xf* infection dynamics were assessed. We checked whether the infection was completely eradicated or not and the spread of the infection, measured in terms of the proportion of infected area under managed conditions compared with the area obtained in the unmanaged epidemiological scenario at the same time horizon.

3. Results

3.1. Disease pressure

The spatio-temporal dynamics of the infection in the simulation scenarios are represented in Fig. 4. The mean disease level in the infected plants decreases with a common pattern over the spatial dimension in the four scenarios (Fig. 4-a). However, only in the Epidem - HH, the mean level of the disease is at least equal to the first level of severity of symptoms outside the area of radius 50-meter from the points of inoculum. In the Epidem - LH and Epidem - LL cases, the mean disease levels never reach the third level of severity of symptoms. The temporal dynamics are then assessed on the worst-case scenario, i.e., the one with the highest average disease pressure. In the Epidem - HH scenario, the mean level of disease in infected plants grows very slowly in the first 3 years of simulation (Fig. 4-b). The threshold of visual detection of symptoms (i.e., severity class of 1) is exceeded in the fourth year of simulation up to 50 m from the inoculation site, in the fifth year symptoms are visible up to 300 m from the inoculation site.

3.2. Infected vector pressure

The mean densities of infected vectors decrease with a common pattern over the spatial dimension in all the simulation scenarios, although the maximum population values are quite different (Fig. 5-b). The temporal dynamics of the density of infected vectors are shown for the scenario Epidem - HH in Fig. 5-a.

In the last year of simulation, the highest mean density of infected vectors for the two scenarios characterized by a low vector abundance is equal to 0.16 (Epidem - HL) and 0.08 (Epidem - LL) vectors per 100 m^2. For the HH scenario, the mean density of infected vectors per 100 m^2 in the last year of simulation is greater than 1 only within the first 500 m from the inoculation point.

3.3. Infected host plants

The annual distributions of infected host plants for each simulation scenario are shown in Fig. 6. The highest number of infected plants (almost 70,000, equal to 6.58% of the host plants in the landscape)

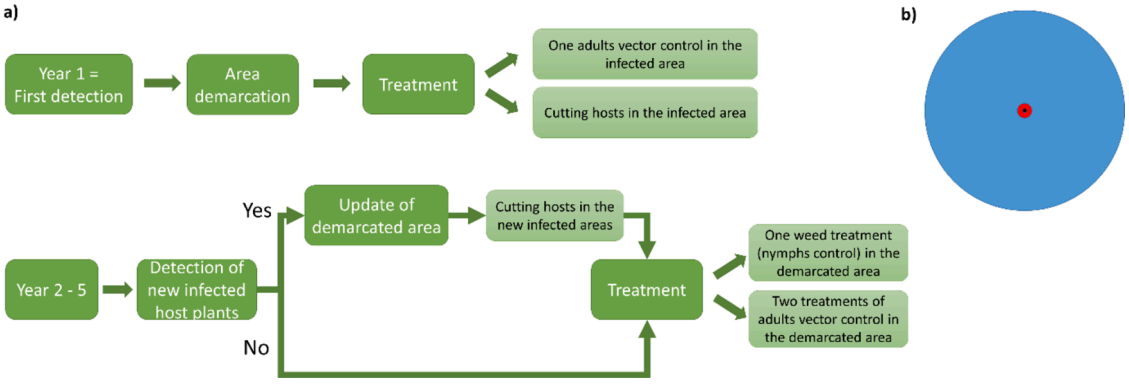

Fig. 3. Overall structure of the management strategy tested in the simulation scenario analysis. On the left (a) is presented the sequence and type of management actions to be implemented according to the simulation year: year 1 is the year in which the first infected plant is detected, from year 2 to year 5 are the following years until the end of the simulation period. On the right (b) is reported the spatial structure of the demarcated area is displayed. The central black dot is the plant detected as infected, the red area is the infected area, and the blue area is the buffer zone.

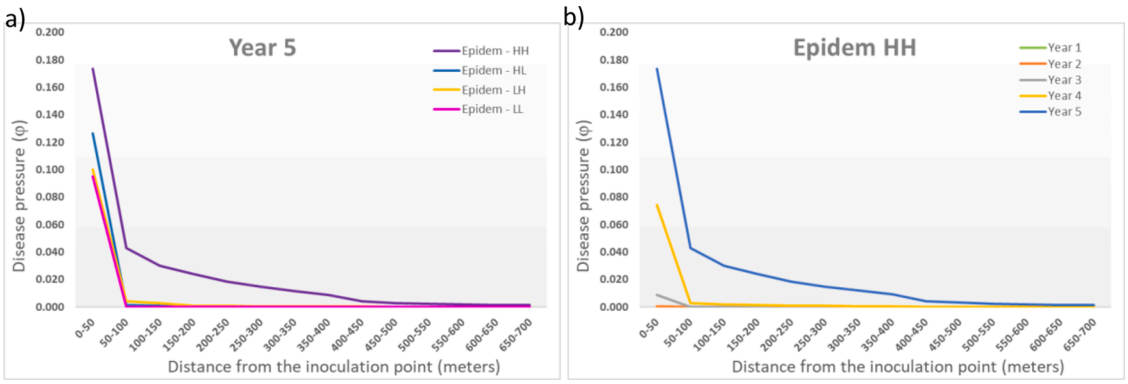

Fig. 4. Distribution of the disease pressure (mean value of the health status of the infected plants) according to the distance from the points of inoculum. a) Scenario comparison: results obtained at the end of the simulation period for the four simulation scenarios. b) Temporal dynamics: results obtained at the end of each of the five simulation years in the scenario HH.
Epidem - HH: High plant susceptibility-High vector abundance; Epidem - HL: High plant susceptibility-Low vector abundance; Epidem - LH: Low plant susceptibility-High vector abundance; Epidem - LL: Low plant susceptibility-Low vector abundance.

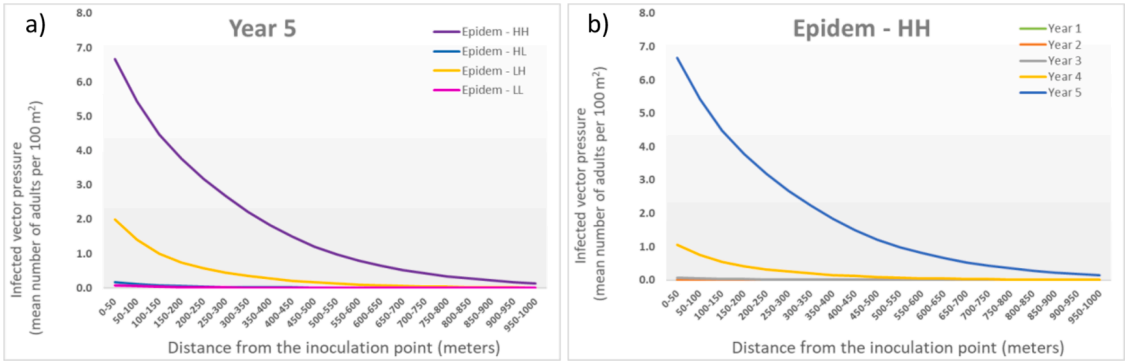

Fig. 5. Distribution of infected vector pressure (mean annual density per 100 m^2 of the population abundance of infected vectors) according to the distance (meters) from the points of inoculum. a) Scenarios comparison: Results obtained in the last year of simulation for the four simulation scenarios. B) Temporal dynamics: Results obtained for the 5 years of simulation in the scenario Epidem - HH.
Epidem - HH: High plant susceptibility-High vector abundance; Epidem - HL: High plant susceptibility-Low vector abundance; Epidem - LH: Low plant susceptibility-High vector abundance; Epidem - LL: Low plant susceptibility-Low vector abundance.

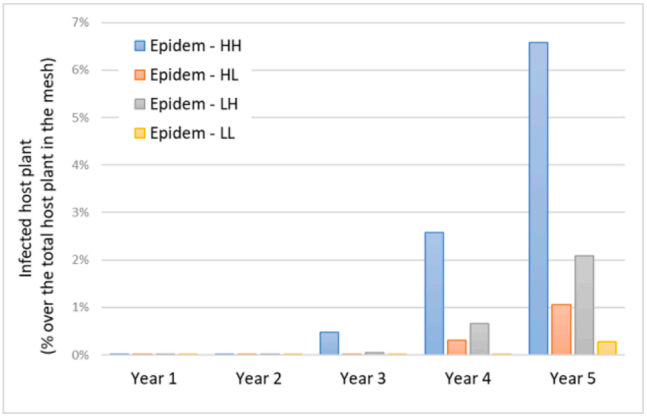

Fig. 6. Distribution of the infected host plants at the end of each simulation year in the four simulation scenarios.

occurred in the scenario Epidem - HH. In the Epidem - LL, there are less than 3000 infected plants at the end of the 5th year of simulation.

3.4. Disease spread

The spread of the infection has been assessed based on the dynamics of the 5 years of simulation, focusing on the initial build-up of an invasion front. At the end of the simulation period, the maximum distance of infected plants from the initial inoculation point is approximately 1500 m for scenario HH, 970 m for LH, 600 m for HL and 340 m for LL. The spread rates for each scenario, expressed as km travelled by the invasion front per year, are reported in Fig. 7. The spread rates increase over time, with different non-linear patterns based on the simulation

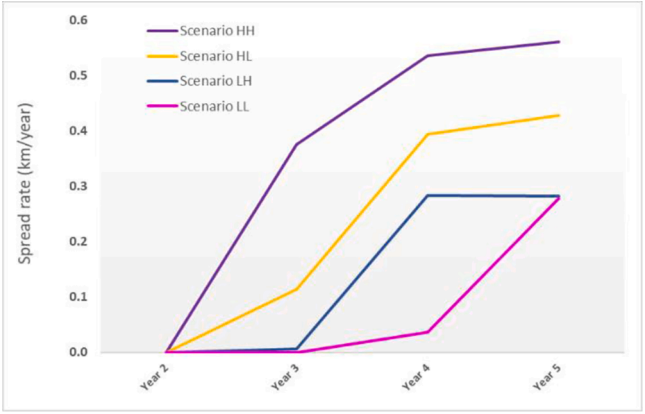

Fig. 7. The spread rate of the disease (km/year) in the four simulation scenarios.

scenario considered. At the end of the simulation period, the spread rate is 0.56 km per year for the scenario HH, 0.43 km per year for LH and about 0.28 km per year for HL and LL.

3.5. Management option efficacy

The basic epidemiological scenario used to define the management strategies was scenario Epidem-HH, high density of vector population and high susceptibility of the host plant to Xf.

The results of the scenario analysis on management strategies are shown in Table 5. In nine of the 16 management scenarios, *Xf* infection was successfully eradicated, with different impacts in terms of the spread of infection depending on the strategy adopted. From the outcomes, the effects of control efficacy, cut radius, time to detection and intervention can be derived.

The greatest effect on eradication is determined by the efficacy of nymphs and adult control treatments. In the eight scenarios where high efficacy of control actions was simulated, the infection was eradicated at the end of the assessment period. In the eight scenarios where control actions have low efficacy, only one management strategy leads to eradication: early detection, early intervention, and a cut radius of 100 m. In all the other management scenarios with low vector control efficacy, eradication is not achieved. Furthermore, in the seven scenarios where eradication is not achieved, the management actions reduce the pressure of the infected vectors to less than 0.035 vectors/m^2.

4. Discussion and conclusion

In XEM, the main biological processes related to the disease dynamics are described in detail, with reference to (i) the vector acquisition of the bacterium from the plant, (ii) the bacterial transmission rate from the vector to the plant, (iii) the growth process of the pathogen inside the plant, and (iv) the vector's dispersal. Rates and functions describing these processes can be adapted to environmental characteristics and host susceptibility. Process functions and parameters can also be adapted to different vector species and *Xf* subspecies or strains.

The application of XEM to the case of the spread of *Xf* in Apulia allowed estimating the spread rate of the infection under the hypothesis that the bacterium is spread by natural vector dispersal only. The disease spread rate increases year by year and reaches about 0.6 km per year 5 years after the initial inoculation. The average annual spread of the infection is expected to be considerably greater if long jumps are considered (Bodino et al., 2021).

A critical issue in dealing with emerging diseases is related to knowledge gaps (Tamborindeguy et al., 2017). The lack of historical data on biological processes makes it difficult to calibrate the models on the analysed system, even when it is possible to describe the dynamics in formal and modeling terms. The estimations of XEM parameters are affected by a set of variability and uncertainty sources related to model assumptions and to the eco-epidemiological system that is studied.

The susceptibility of plants influences the growth rate of the bacterial population in the plant, and it has a significant impact on the duration of the asymptomatic period. The XEM allows for the evaluation of the progression of the disease in the plants. The possibility of defining specific growth rates for different periods of the year (to account for plant phenology and environmental conditions) and host plant susceptibilities (among species or individuals within the same species), allows for the application of XEM to several agroecosystems. Furthermore, associating the host plant health status with a scale of symptoms onset allows for modeling any type of disease latency (i.e., the period in which the pathogen is present in the plant, but it is not detectable, neither visually nor with laboratory diagnostic procedures). The calibration of XEM parameters related to disease growth and latency period requires knowledge on the susceptibility of the host plants/cultivars of interest and the specific bacterial growth mechanisms within these species. Recent studies are bringing evidence regarding the importance of weeds in the *Xf*-olive tree-vector pathosystem, as they represent both the habitat where the vector nymphs complete their development and a possible reservoir for the bacterium (Aniţa et al., 2021; Brunetti et al., 2020). In our study, the herbaceous plant community has been considered only as support in the pre-imaginal stage development. Further developments of the model may include the weeds as a potential host for the bacterium in order to assess their contribution to the epidemiology of *Xf*-olive tree-vector pathosystem.

The variability related to vector spread rate and dispersal patterns can be addressed by modifying the uncertainty distribution for the vector dispersal kernel. A different spread rate or a non-homogenous distribution of the disease could have direct effects on the assessment of spatio-temporal dynamics of disease spread and, therefore, on the assessment of management or eradication strategies.

The vector acquisition rate can be modified to consider the within- and between-species variability in the feeding rate and preference.

The density of the vector population is highly variable. Since the scenario results showed that it had a strong impact on *Xf* spread, actions aimed to strongly reduce vector population abundance could be key elements for the success of eradication strategies. For these reasons, careful studies to estimate the abundance of the population should be preliminary to the implementation of the XEM model.

Table 5
Results of the simulation scenarios on management strategies for the infection of *Xylella fastidiosa*.

Factors and levels					Simulation scenario 5 years after detection	
Management Scenario	**Control efficacy**	**Detection**	**Time to intervention**	**Cut radius**	**Successfully eradication**	**Percentage of infected area***
Manag-01	High	Early	Early	Large	Yes	13.0%
Manag-02				Small		10.8%
Manag-03			Late	Large		13.2%
Manag-04				Small		11.9%
Manag-05		Late	Early	Large		18.2%
Manag-06				Small		15.4%
Manag-07			Late	Large		18.3%
Manag-08				Small		18.0%
Manag-09	Low	Early	Early	Large		13.4%
Manag-10	Low	Early	Early	Small	No	14.7%
Manag-11			Late	Large		19.0%
Manag-12				Small		17.9%
Manag-13		Late	Early	Large		22.3%
Manag-14				Small		22.1%
Manag-15			Late	Large		27.0%
Manag-16				Small		23.0%

* Percentage of infected area compared to the area of infection detected at the same time horizon in the unmanaged epidemiological scenario (Epidem-HH): the 8th and 9th year of epidemiological simulation for early and late detection, respectively.

In scenario analysis of epidemiological dynamics, the rate of successful transmission of the pathogen from the infected vector to the host plant and from an infected plant to the vector are among the parameters that most influence system dynamics. The results of new experimental studies on these factors could easily be included in XEM.

The generality and flexibility of XEM make the model a suitable tool to better understand the disease mechanisms and patterns and to evaluate the effectiveness of different risk reducing options and practices devoted to the management of the disease pressure and spread. XEM can also be used for the evaluation of management and/or eradication strategies. In our scenario analysis, the high efficacy of vector and weed control intervention are identified as the key factors for a successful eradication (in accordance with Aniţa et al. (2021). The prompt intervention after infection detection could limit the impact of *XF* when eradication is not achieved. From simulation outcomes, it emerges that the management measures are effective if performed just after adults' emergence (early intervention) limiting the density of infected vectors that rapidly increases over the favourable season. This result is an example of useful information to support decision-making as it underlines the importance of limiting the delay in applying control actions, other things being equal, in the system considered.

The cut-off radius is crucial for eradication only when there is early detection and timely intervention, and the efficacy of vector control is low. In these scenarios, the 100 m cut radius allows achieving the eradication, whereas a smaller radius (50 m) does not allow this.

The management strategies influence the infection spread, measured in the percentage of the infected area compared to the infected area in the unmanaged scenario. In particular, lower infected areas occur in all the scenarios with early detection. In the scenarios where eradication is not achieved, the spread of infection can be reduced by reducing the time of application of intervention measures (early intervention).

From the analyses carried out, it emerges that further knowledge is needed on the main sources of uncertainty in the eco-epidemiological system analysed, in particular the susceptibility of the host plants, the rate at which the bacteria are acquired by the vector, the range of movement of the vector and the delay in detecting the disease.

XEM could be used to assess the outcome of the application of different detection and control strategies. Each process described in XEM (e.g., vector-plant transmission, asymptomatic period, growth of the bacterium into the plant, vector phenology) is defined by specific parameters. The inclusion in the model of detection/control strategies is simplified and requires only the estimation of the impact that these actions have on related parameters of the model (e.g., a control action of the vector will reduce the carrier's carrying capacity). Being spatially explicit, XEM allows assessing the impact of actions only in the areas where they are implemented. Furthermore, the temporal resolution of the model and the inclusion of the phenology of both host plants and vectors allows the evaluation of the variability of the efficacy of the detection/control strategies according to the period in which they are carried out.

The huge efforts and investments in research on *Xf* led to an increasing amount of knowledge on both the bacterium (e.g., the basic mechanisms of disease infection and growth in the host plant) and the vectors (e.g., phenology). However, this knowledge body of growing complexity urgently needs integration into efficient and readily available tools to support strategies for preventing and mitigating the effects of *Xf*. These tools should be able to stock up on low-scale (e.g., i-state model) to high-scale (p-state model) knowledge (Gyllenberg, 2007; Caswell and John, 1992). XEM allows integrating the scientific evidence at various spatial and temporal resolutions (from individual plants to large-scale heterogeneous landscapes), including the effects of environmental drivers (climate and land use) and climate change. Therefore, XEM could be implemented in control strategies for *Xf* management at different levels, from field to regional, from operational to policy, supporting the implementation of risk reduction options in plant health and for selecting control techniques and guiding the development of IPM strategies at the farm- and area-wide-level.

CRediT authorship contribution statement

Gianni Gilioli: Conceptualization, Formal analysis, Methodology, Software, Writing – review & editing, Supervision. **Anna Simonetto:** Conceptualization, Formal analysis, Data curation, Methodology, Software, Validation, Writing – original draft, Writing – review & editing. **Michele Colturato:** Software, Writing – review & editing. **Noelia Bazarra:** Software, Writing – review & editing. **José R. Fernández:** Software, Writing – review & editing. **Maria Grazia Naso:** Software, Writing – review & editing. **Boscia Donato:** Conceptualization, Writing – review & editing. **Domenico Bosco:** Conceptualization, Writing – review & editing. **Crescenza Dongiovanni:** Conceptualization, Writing – review & editing. **Andrea Maiorano:** Conceptualization, Writing – review & editing. **Olaf Mosbach-Schulz:** Conceptualization, Writing – review & editing. **Juan A. Navas Cortés:** Conceptualization, Writing – review & editing. **Maria Saponari:** Conceptualization, Writing – review & editing.

Declaration of Competing Interest

The authors declare the following financial interests/personal relationships which may be considered as potential competing interests: Maiorano Andrea and Mosbach-Schulz Olaf report a relationship with European Food Safety Authority (EFSA) that includes: employment. The authors Maiorano Andrea and Mosbach-Schulz Olaf write under their own name and the article engages themselves and not the responsibility of EFSA. The views or positions expressed in this publication do not necessarily represent in legal terms the official position of the European Food Safety Authority (EFSA). EFSA assumes no responsibility or liability for any errors or inaccuracies that may appear

Data Availability

Data will be made available on request.

References

Almeida, R.P.P., Wistrom, C., Hill, B.L., Hashim, J., Purcell, A.H., 2005. Vector transmission of *Xylella fastidiosa* to dormant grape. Plant Dis. 89 (4), 419–424. https://doi.org/10.1094/PD-89-0419.

Aniţa, S., Capasso, V., Scacchi, S., 2021. Controlling the spatial spread of a Xylella epidemic. Bull. Math. Biol. 83 (4), 32. https://doi.org/10.1007/s11538-021-00861-z.

Bazarra, N., Colturato, M., Fernández, J.R., Naso, M.G., Simonetto, A., Gilioli, G., 2022. Analysis of a mathematical model arising in plant disease epidemiology. Applied Mathematics & Optimization 85 (2), 19. https://doi.org/10.1007/s00245-022-09858-z.

Bodino, N., Cavalieri, V., Dongiovanni, C., Plazio, E., Saladini, M.A., Volani, S., Simonetto, A., Fumarola, G., Carolo, M.D., Porcelli, F., Gilioli, G., Bosco, D., 2019. Phenology, seasonal abundance and stage-structure of spittlebug (Hemiptera: aphrophoridae) populations in olive groves in Italy. Sci. Rep. 9 (1), 17725. https://doi.org/10.1038/s41598-019-54279-8.

Bodino, N., Cavalieri, V., Dongiovanni, C., Saladini, M.A., Simonetto, A., Volani, S., Plazio, E., Altamura, G., Tauro, D., Gilioli, G., Bosco, D., 2020. Spittlebugs of Mediterranean olive groves: host-plant exploitation throughout the year. Insects 11 (2), 130. https://doi.org/10.3390/insects11020130.

Bodino, N., Cavalieri, V., Dongiovanni, C., Simonetto, A., Saladini, M.A., Plazio, E., Gilioli, G., Molinatto, G., Saponari, M., Bosco, D., 2021a. Dispersal of Philaenus spumarius (Hemiptera: aphrophoridae), a vector of Xylella fastidiosa, in olive grove and meadow agroecosystems. Environ. Entomol. 50 (2), 267–279. https://doi.org/10.1093/ee/nvaa140.

Bodino, N., Demichelis, S., Simonetto, A., Volani, S., Saladini, M.A., Gilioli, G., Bosco, D., 2021b. Phenology, seasonal abundance, and host-plant association of spittlebugs (Hemiptera: aphrophoridae) in vineyards of Northwestern Italy. Insects 12 (11). https://doi.org/10.3390/insects12111012. Art11.

Brezis, H., 1986. Liguori Editore Srl. Analisi funzionale: Teoria e applicazioni, 9.

Brunetti, M., Capasso, V., Montagna, M., Venturino, E., 2020. A mathematical model for Xylella fastidiosa epidemics in the Mediterranean regions. Promoting good agronomic practices for their effective control. Ecol. Modell. 432, 109204 https://doi.org/10.1016/j.ecolmodel.2020.109204.

Caswell, H., & John, A.M. (1992). From the individual to the population in demographic models. In *Individual-Based Models and Approaches in Ecology*. Chapman and Hall/CRC.

Cavalieri, V., Altamura, G., Fumarola, G., di Carolo, M., Saponari, M., Cornara, D., Bosco, D., Dongiovanni, C., 2019. Transmission of Xylella fastidiosa subspecies pauca sequence type 53 by different insect species. Insects 10 (10). https://doi.org/10.3390/insects10100324. E324.

Chapman, D., White, Steven, Hooftman, Danny A.P., & Bullock, James. (2015). Inventory and Review of Quantitative Models For Spread of Plant Pests For Use in Pest Risk Assessment For the EU Territory. EFSA Supporting Pubblication, 190.

Cavalieri, V., Porcelli, F., 2017. Main insect vectors of Xylella fastidiosa in Italy and worldwide. Xylella fastidiosa & the Olive Quick Decline Syndrome (OQDS): A serious worldwide challenge for the safeguard of olive trees. In: D'Onghia, A.M., Brunel, S., Valentini, F. (Eds.), , Options Méditerranéennes : Série A. Séminaires Méditerranéens121. CIHEAM, Bari, pp. 31–32.

Cornara, D., Bosco, D., Fereres, A., 2018. Philaenus spumarius: when an old acquaintance becomes a new threat to European agriculture. J. Pest Sci. (2004) 91 (3), 957–972. https://doi.org/10.1007/s10340-018-0966-0.

Cornara, D., Cavalieri, V., Dongiovanni, C., Altamura, G., Palmisano, F., Bosco, D., Porcelli, F., Almeida, R.P.P., Saponari, M., 2017. Transmission of *Xylella fastidiosa* by naturally infected *Philaenus spumarius* (Hemiptera, Aphrophoridae) to different host plants. J. Appl. Entomol. 141 (1–2), 80–87. https://doi.org/10.1111/jen.12365.

Council Directive 2000/29/EC, (2000). http://data.europa.eu/eli/dir/2000/29/oj/eng.

Cruaud, A., Gonzalez, A.-.A., Godefroid, M., Nidelet, S., Streito, J.-.C., Thuillier, J.-.M., Rossi, J.-.P., Santoni, S., Rasplus, J.-.Y., 2018. Using insects to detect, monitor and predict the distribution of Xylella fastidiosa: a case study in Corsica. Sci. Rep. 8 (1), 15628. https://doi.org/10.1038/s41598-018-33957-z.

Decision (EU) 2015/789, COM (2015). http://data.europa.eu/eli/dec_impl/2015/789/oj/eng.

Decision (EU) 2017/2352, SANTE, COM (2017). http://data.europa.eu/eli/dec_impl/2017/2352/oj/eng.

Di Serio, F., Bodino, N., Cavalieri, V., 2019. Collection of Data and Information On Biology and Control of Vectors of Xylella fastidiosa, 102. EFSA Supporting Publication. https://doi.org/10.2903/sp.efsa.2019.EN-1628. *EN-1628*.

EFSA PLH Panel, 2019. Update of the Scientific Opinion on the risks to plant health posed by Xylella fastidiosa in the EU territory. EFSA J. 200.

EFSA PLH Panel, 2020. Update of the Xylella spp. Host plant database – systematic literature search up to 30 June 2019. EFSA J. 61.

EPPO Reporting Service. (2018). *Xylella fastidiosa eradicated from Switzerland* (Fasc. 083). European and Mediterranean Plant Protection Organization.

EPPO Reporting Service. (2019). *Xylella fastidiosa subsp. Multiplex was first found in December 2018 on lavender plants (in a zoo garden) in the municipality of Vila Nova de Gaia (near Porto)* (Fasc. 017). European and Mediterranean Plant Protection Organization.

REGULATION (EU) 2020/1201, fasc. REGULATION (EU) 2020/1201 (2020). https://eur-lex.europa.eu/legal-content/EN/TXT/PDF/?uri=CELEX:32020R1201&from=en.

Fierro, A., Liccardo, A., Porcelli, F., 2019. A lattice model to manage the vector and the infection of the Xylella fastidiosa on olive trees. Sci. Rep. 9 (1), 8723. https://doi.org/10.1038/s41598-019-44997-4.

Giampetruzzi, A., Morelli, M., Saponari, M., Loconsole, G., Chiumenti, M., Boscia, D., Savino, V.N., Martelli, G.P., Saldarelli, P., 2016. Transcriptome profiling of two olive cultivars in response to infection by the CoDiRO strain of Xylella fastidiosa subsp. Pauca. BMC Genomics 17, 475. https://doi.org/10.1186/s12864-016-2833-9.

Gyllenberg, M., 2007. Mathematical aspects of physiologically structured populations: the contributions of J. A. J. Metz. J. Biol. Dyn. 1 (1), 3–44. https://doi.org/10.1080/17513750601032737.

Hopkins, D.L., Purcell, A.H., 2002. Xylella fastidiosa: cause of Pierce's disease of grapevine and other emergent diseases. Plant Dis. 86 (10), 1056–1066. https://doi.org/10.1094/PDIS.2002.86.10.1056.

Ivlev, V.S., 1961. Experimental Ecology of the Feeding of Fishes. Yale University Press.

Jeger, M., Bragard, C., 2019. The epidemiology of Xylella fastidiosa ; a perspective on current knowledge and framework to investigate plant host–vector–pathogen interactions. Phytopathology® 109 (2), 200–209. https://doi.org/10.1094/PHYTO-07-18-0239-FI.

Lopes, J.R.S., Daugherty, M.P., Almeida, R.P.P., 2009. Context-dependent transmission of a generalist plant pathogen: host species and pathogen strain mediate insect vector competence. Entomol. Exp. Appl. 131 (2), 216–224. https://doi.org/10.1111/j.1570-7458.2009.00847.x.

Montes-Borrego, M., Boscia, Donato, Landa, Blanca B., Saponari, Maria, & Navas-Cortés, J.A. (2017). *Spatial and temporal dynamics of olive quick decline syndrome in orchards in Puglia, southern Italy. European Conference on Xylella fastidiosa: Finding answers to a global problem*. European conference on Xylella fastidiosa: finding answers to a global problem, Palma de Mallorca.

Moralejo, E., Borràs, D., Gomila, M., Montesinos, M., Adrover, F., Juan, A., Nieto, A., Olmo, D., Seguí, G., Landa, B.B., 2019. Insights into the epidemiology of Pierce's disease in vineyards of Mallorca, Spain. Plant Pathol. 68 (8), 1458–1471. https://doi.org/10.1111/ppa.13076.

Nunney, L., Vickerman, D.B., Bromley, R.E., Russell, S.A., Hartman, J.R., Morano, L.D., Stouthamer, R., 2013. Recent evolutionary radiation and host plant specialization in the Xylella fastidiosa subspecies native to the United States. Appl. Environ. Microbiol. 79 (7), 2189–2200. https://doi.org/10.1128/AEM.03208-12.

Parnell, S., van den Bosch, F., Gottwald, T., Gilligan, C.A., 2017. Surveillance to inform control of emerging plant diseases: an epidemiological perspective. Annu. Rev. Phytopathol. 55 (1), 591–610. https://doi.org/10.1146/annurev-phyto-080516-035334.

Perring, T., Farrar, C., Blua, M., 2001. Proximity to citrus influences Pierce's disease in Temecula Valley vineyards. Calif Agric (Berkeley) 55 (4), 13–18.

Purcell, A.H., Saunders, S.R., Hendson, M., Grebus, M.E., Henry, M.J., 1999. Causal role of Xylella fastidiosa in oleander leaf scorch disease. Phytopathology® 89 (1), 53–58. https://doi.org/10.1094/PHYTO.1999.89.1.53.

Mizell III, R. F. Redak, R.A., Purcell, A.H., Lopes, J.R.S., Blua, M.J., Andersen, P.C, 2004. The biology of xylem fluid-feeding insect vectors of Xylella fastidiosa and their relation to disease epidemiology Annu. Rev. Entomol. 49 (1), 243–270. https://doi.org/10.1146/annurev.ento.49.061802.123403.

Sanderlin, R.S., 2017. Host specificity of pecan strains of Xylella fastidiosa subsp. Multiplex. Plant Dis. 101 (5), 744–750. https://doi.org/10.1094/PDIS-07-16-1005-RE.

Saponari, M., Boscia, D., Altamura, G., Loconsole, G., Zicca, S., D'Attoma, G., Morelli, M., Palmisano, F., Saponari, A., Tavano, D., Savino, V.N., Dongiovanni, C., Martelli, G. P., 2017. Isolation and pathogenicity of Xylella fastidiosa associated to the olive quick decline syndrome in southern Italy. Sci. Rep. 7 (1), 17723. https://doi.org/10.1038/s41598-017-17957-z.

Saponari, M., Giampetruzzi, A., Loconsole, G., Boscia, D., Saldarelli, P., 2019a. *Xylella fastidiosa* in Olive in Apulia: where we stand. Phytopathology® 109 (2), 175–186. https://doi.org/10.1094/PHYTO-08-18-0319-FI.

Saponari, M., Loconsole, G., & Nigro, F. (2019b). *Knowledge of the pathogenicity and virulence of Xylella fastidiosa subsp. Pauca ST53 on susceptible—Deliverable 2.1—H2020 POnTE project*. https://www.ponteproject.eu/wp-content/uploads/2019/04/Deliverable-2.1_Knowledge-of-the-pathogenicity-and-virulence-of-Xylella-fastidiosa-subsp.-pauca-ST53-on-susceptible-hosts_REVREV.pdf.

Schneider, K., van der Werf, W., Cendoya, M., Mourits, M., Navas-Cortés, J.A., Vicent, A., Lansink, Oude, 2020. Impact of Xylella fastidiosa subspecies pauca in European olives. Proc. Nat. Acad. Sci. 117 (17), 9250–9259. https://doi.org/10.1073/pnas.1912206117.

Sicard, A., Zeilinger, A.R., Vanhove, M., Schartel, T.E., Beal, D.J., Daugherty, M.P., Almeida, R.P.P., 2018. Xylella fastidiosa: insights into an Emerging Plant Pathogen. Annu. Rev. Phytopathol. 56 (1), 181–202. https://doi.org/10.1146/annurev-phyto-080417-045849.

Strona, G., Carstens, C.J., Beck, P.S.A., 2017. Network analysis reveals why Xylella fastidiosa will persist in Europe. Sci. Rep. 7 (1), 71. https://doi.org/10.1038/s41598-017-00077-z.

White, S., Bullock, J., Cavers, S., & Chapman, Daniel. (2019). *PHC2018/05—Using modelling to investigate the effectiveness of national surveillance monitoring aimed at detecting a Xylella fastidiosa outbreak in Scotland* (p. 22). Plnt Health Centre, Scotland's Centre of Expertise.

White, S.M., Bullock, J.M., Hooftman, D.A.P., Chapman, D.S., 2017. Modelling the spread and control of Xylella fastidiosa in the early stages of invasion in Apulia, Italy. Biol. Invasions 19 (6), 1825–1837. https://doi.org/10.1007/s10530-017-1393-5.

White, S.M., Navas-Cortés, J.A., Bullock, J.M., Boscia, D., Chapman, D.S., 2020. Estimating the epidemiology of emerging *Xylella fastidiosa* outbreaks in olives. Plant Pathol. https://doi.org/10.1111/ppa.13238 ppa.13238.